


MINI-SYMPOSIUM: RECENT ADVANCES IN NEUROIMAGING IN MULTIPLE SCLEROSIS, AND THEIR EUROPEAN HISTORICAL SIGNIFICANCE

Iron related changes in MS lesions and their validity to characterize MS lesion types and dynamics with Ultra-high field magnetic resonance imaging

Simon Hametner^{1,2}, Assunta Dal Bianco^{1,3}, Siegfried Trattinig⁴ and Hans Lassmann¹ 

¹ Center for Brain Research, Medical University of Vienna, Austria

² Institute of Neuropathology, University of Göttingen, Germany

³ Department of Neurology, Medical University of Vienna, Austria

⁴ Department of Biomedical Imaging and Image-guided Therapy, High Field Magnetic Resonance Center, Medical University of Vienna, Austria.

Keywords

iron, magnetic resonance imaging, multiple sclerosis, pathology

Corresponding author:

Prof. Dr. Hans Lassmann, Center for Brain Research, Medical University of Vienna, Spitalgasse 4, A-1090 Wien, Austria (E-mail: hans.lassmann@medunivwien.ac.at)

Received 6 June 2018

Accepted 12 June 2018.

doi:10.1111/bpa.12643

Abstract

Iron accumulates with age in the normal human brain. This process is altered at several levels in the brain of multiple sclerosis (MS) patients. Since iron is mainly stored in oligodendrocytes and myelin in the normal brain, its liberation in demyelinating lesions may amplify tissue damage in demyelinating lesions and its uptake in macrophages and microglia may help to more precisely define activity stages of the lesions. In addition, glia cells change their iron import, export and storage properties in MS lesions, which is reflected by alterations in the expression of iron transport molecules. Changes of iron distribution in the brain can be reliably detected by MRI, particularly upon application of Ultra-high magnetic field (7 Tesla). Iron-sensitive MRI allows to more accurately distinguish the lesions in MS from those in other inflammatory brain diseases, to visualize a subset of slowly expanding lesions in the progressive stage of MS and to increase the sensitivity for lesion detection in the grey matter, such as the cerebral cortex or deep grey matter nuclei.

INTRODUCTION

Multiple sclerosis (MS) is a chronic inflammatory disease of the central nervous system, which leads to the formation of focal plaques with primary demyelination and neurodegeneration within the lesions and in the normal appearing white and grey matter. While basic mechanisms of the inflammatory process have been well elucidated during the last decades and a large spectrum of anti-inflammatory or immunomodulatory treatments are currently available, much less is known about the molecular mechanisms responsible for the induction of demyelination and neurodegeneration. We have recently proposed that tissue damage in multiple sclerosis is primarily driven by components of the adaptive and innate immune system, and that oxidative injury and subsequent mitochondrial damage plays a major pathogenic role in the disease (40). Oxidative injury can be amplified by the presence of iron in the human brain and by its liberation within the lesions. For this reason, a detailed insight into the dynamic changes of iron metabolism in the brain of normal humans and MS patients may allow to identify novel mechanisms, which propagate neurodegeneration in MS. These mechanisms may be particularly important in aging patients with progressive disease. Furthermore, the introduction of Ultra-high field (7 Tesla) magnetic resonance imaging provides improved resolution and contrast in MRI

to study disease-related iron homeostasis *in vivo* in the brain of MS patients, and such data may become clinically relevant for diagnosis, prognosis and the evaluation of therapeutic success. In this review, we briefly discuss neuropathological evidence for iron related changes in the brain and provide a summary of the current state of the art of iron-sensitive magnetic resonance imaging in MS patients.

IRON IN THE NORMAL BRAIN

In mammalian organisms, iron is present in two forms: heme iron and non-heme iron. Heme iron is functional, i.e. used for metabolic purposes, and a major pool of divalent (Fe^{2+}) heme iron is found as a prosthetic group of highly concentrated intracellular hemoglobin in erythrocytes. Conversely, concentrations of extracellular free hemoglobin in the serum are normally low. Upon hemolysis, large amounts of hemoglobin can be liberated, which might have deleterious effects due to the pro-oxidative abilities of heme. For these reasons, the abundant serum protein haptoglobin binds and detoxifies hemoglobin via intravascular sequestration and uptake into monocytes (50) through the hemoglobin-haptoglobin complex receptor CD163 (35). Scavenged hemoglobin is degraded in

lysosomes, and iron is removed from liberated heme via heme oxygenases. The remaining protoporphyrin IX ring is further degraded to biliverdin and carbon monoxide (19). In the body, heme iron contributes to about 75% of the total iron pool (3.5 g heme iron and 4.5 g total iron in a 70 kg man).

Non-heme iron includes all iron which is not found in heme. It can be functional if it is e.g. present in iron-sulfur clusters, or non-functional if it is stored in ferritin or bound to transferrin. It also subsumes free iron, which is normally found in the intracellular labile or chelatable iron pool (13). Cellular Fe²⁺ is imported across the cytoplasmic membrane or membranes of phagosomes and lysosomes by a variety of ion channels, such as DMT1, TRP6, ZIP8, ZIP14, TRPML1 and NRAMP1. Cellular Fe²⁺ export is mediated by the iron channel ferroportin, which is coupled to the copper-dependent ferroxidases hephaestin or ceruloplasmin (28). These membrane-bound ferroxidases oxidize Fe²⁺ to Fe³⁺ directly after export via ferroportin, preventing the cellular release of toxic divalent iron into the extracellular space. Cells import Fe³⁺ via receptor-mediated endocytosis of iron-containing transferrin or ferritin via receptors for transferrin (TfR1) or ferritin (Scara5 (38), Tim-1 (9)).

The human brain accumulates iron with aging (22). Areas showing pronounced iron accumulation are the basal ganglia, the substantia nigra, the red nucleus, the cerebellar dentate nucleus and the cortico-subcortical junction. In the deep and periventricular white matter, iron accumulation is less prominent. A similar anatomical iron distribution is seen in brains of aging rodents, but overall iron levels are much lower than in humans (53). Throughout all brain regions, iron is mainly stored in ferritin in oligodendrocytes and myelin. Conversely, high iron content in few microglia is found only in a subset of aged individuals. Larger numbers of iron-laden microglia and macrophages are found in pathological conditions of the brain, such as Alzheimer's disease (39) or multiple sclerosis (11). Under such circumstances, iron-laden microglia display a senescent phenotype (23), suggesting detrimental effects of long-term iron storage in microglia (Figure 1).

Currently, the mechanisms mediating life-long accumulation of iron in its distinct anatomical pattern remain to be clarified. Iron may enter the brain through a specific receptor-mediated transport (14) and unspecifically under conditions of blood-brain-barrier injury. The destination of iron in oligodendrocytes may be accomplished by the expression of iron importers, such as the ferritin receptor Tim-1 (9), and by the low expression of iron exporters in these cells in comparison to neurons and other glial cells. This, however, does not explain the anatomical distribution of iron accumulation. Age-related vascular pathology and extravasation of erythrocytes or their contents may play an additional role. This concept is supported by the high iron accumulation in the brain at predilection sites of deep hemorrhages associated with hypertensive small vessel disease, which involve lenticulostriate branches of the middle cerebral artery (49).

CHANGES OF IRON METABOLISM IN THE MULTIPLE SCLEROSIS BRAIN

Compared to age matched controls, increased amounts of iron have been observed in the basal ganglia of MS patients already in early disease stages (31). In MS with long-standing disease however, the iron levels of the myelinated normal-appearing white matter (NAWM) are decreased in comparison to controls (23,48). This iron decrease was related to disease duration (23) or age (48) of the patients. As in aging controls, iron in the NAWM and normal-appearing grey matter (NAGM) is mainly stored in myelin and oligodendrocytes, while active or chronic active lesions may contain high and variable numbers of iron-loaded macrophages and a low and variable presence in astrocytes (23,48). In the vicinity of active lesions, the iron content of oligodendrocytes is reduced and this process is associated with the upregulated expression of molecules involved in cellular iron export, such as hephaestin (15), ceruloplasmin (23) and ferroportin. In lesions showing active demyelination, residual iron is liberated from degenerating oligodendrocytes, where it is found in the extracellular space (23) and with advancing lesion formation taken up by macrophages and microglia. These data suggest that liberation of pro-oxidant Fe²⁺ in active MS lesions may amplify oxidative injury of remaining myelin sheaths, oligodendrocytes and axons, leading to the formation of oxidized phospholipids and DNA (23). Iron uptake in microglia may augment microglial senescence (39), which is prominent in MS lesions (23). Upon removal of iron containing macrophages and microglia, chronic inactive lesions are characterized by a reduction in iron content, when compared with surrounding NAWM (23, 48) or NAGM (48, 61). As will be discussed below, this reduced iron content in inactive lesions might be useful for cortical lesion detection with high-field MRI.

Slowly expanding or smoldering lesions show continuing low-grade myelin breakdown and phagocytosis at the lesion edges, which are particularly prevalent in patients with primary or secondary progressive MS (17). In a subset of about 40% of such lesions (23, 48), iron is taken up by activated microglia at the lesion edge, and this results in the appearance of a narrow but prominent rim of iron containing microglia at the smoldering lesion edge (11). Iron-loaded microglia revealed an activated and pro-inflammatory phenotype, signified by the expression of molecules involved in oxygen (11) or nitrogen (42) radical production, phagocytosis and antigen presentation (11, 63). As discussed below, visualization of iron rim lesions by MRI helps to identify slowly expanding lesions in MS patients and may serve as a paraclinical marker for active disease in the progressive stage of MS in the future. These iron-related findings in the MS brain have originally been established by conventional neuropathology using histochemical methods of iron detection (23). More recently, they have been confirmed and expanded using synchrotron X-ray fluorescence imaging (48). This study additionally

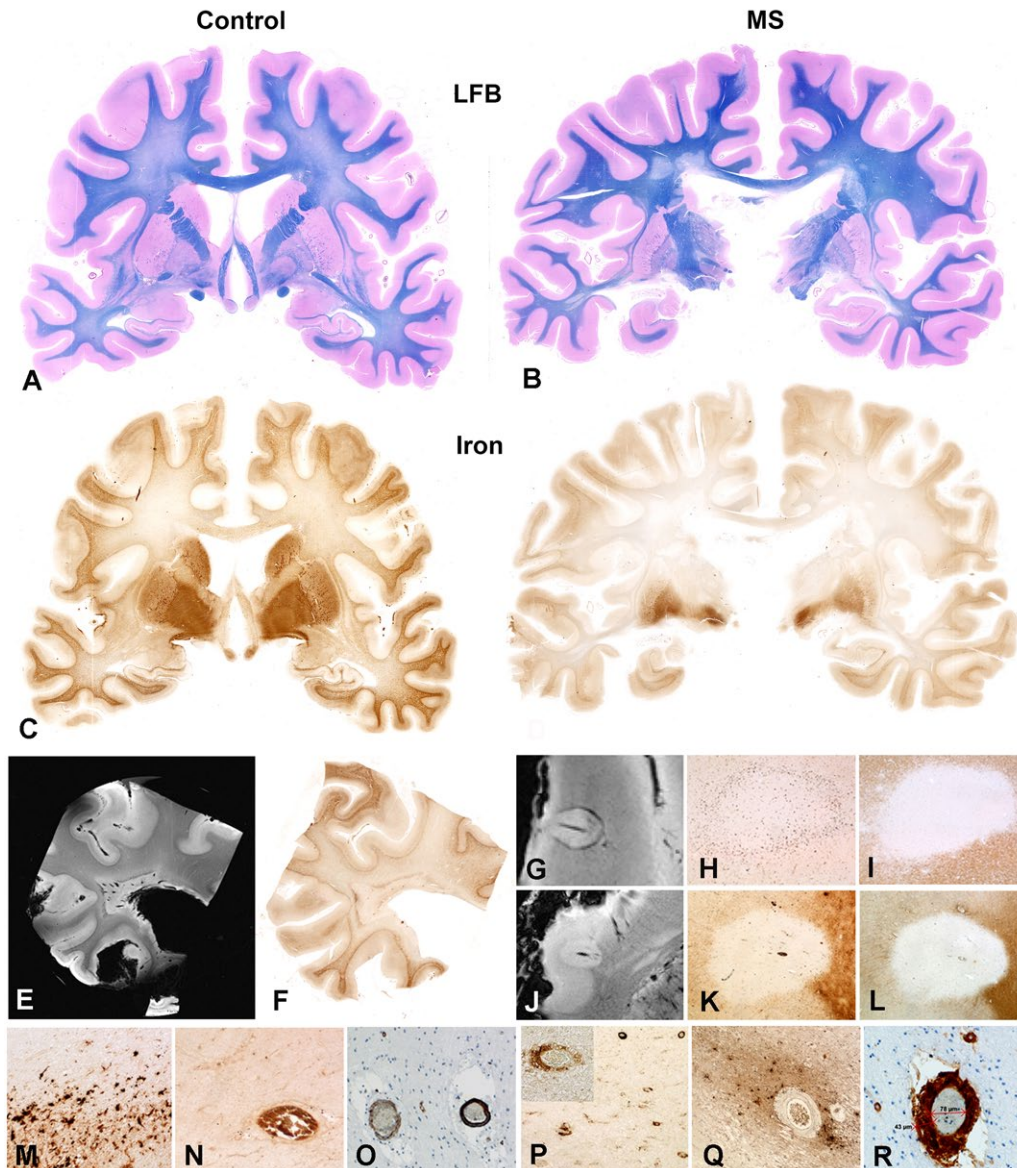


Figure 1. Distribution of iron in control and MS brains and its visualization using 7T MRI. **(A, B)** Luxol-fast blue-periodic acid-Schiff stainings for myelin and **(C, D)** diaminobenzidine-enhanced Turnbull blue stainings for non-heme iron show double-hemispheric coronal sections of **(A, C)** a 63-year old control and **(B, C)** a 55-year old patient with secondary progressive MS. **(B)** Multiple remyelinated shadow plaques are visible in the periventricular and subcortical white matter of the MS case. **(C, D)** In both control and MS case, the highest iron intensities are found in the deep grey matter nuclei and the substantia nigra. The cortico-subcortical junction is also accentuated by elevated iron intensities. **(D)** This MS case shows overall iron reduction in the normal-appearing white matter (NAWM) and even more within the shadow plaques. None of the shadow plaques display a rim of iron accumulation. **(E-L)** 7T susceptibility-weighted imaging (SWI) **(E, G, J)**, iron stainings **(F, H, K)** and proteolipid protein (PLP) myelin stainings **(I, L)** of a 62-year old patient with primary progressive MS. **(E)** The large periventricular lesion is hyperintense when compared to the surrounding NAWM and is bordered by a narrow hypointense rim. **(F)** The hypointense rim is recapitulated by intense iron reactivity within microglia **(M)**. Within the lesion, strongly hypointense tubular structures **(E)** correspond to intravascular erythrocytes in vessels lacking perivascular iron accumulation **(N)**. **(G, H, I)** A leukocortical lesion with a dark rim and central vessel in the SWI sequence **(G)**. The iron staining confirms iron accumulation at the rim **(H)**, and PLP myelin staining confirms myelin loss **(I)**. The central vessel is not captured in the histology. **(J-L)** A leukocortical lesion with a central hypointense vessel without hypointense rim **(J)** and without rim iron accumulation **(K)**. The area of myelin loss is shown in the PLP staining in **(L)** and is characterized by iron loss when compared to the surrounding normal-appearing grey matter **(K)**, which augments the slight hyperintensity of the lesional area in the SWI sequence **(J)**. Here, the central vessel is captured by histology **(K, L)** and displays dark intravascular erythrocytes and no evidence of perivascular iron accumulation **(K)**. **(O)** Staining for smooth muscle actin allows to differentiate between veins (left vessel) and arteries (right vessel). **(P)** Perivascular iron accumulation within a chronic MS lesion within macrophages in the perivascular spaces can be differentiated from **(Q)** periarterial iron accumulation, which diffuses into the neighbouring brain parenchyma within another chronic MS lesion. **(R)** Vascular fibrosis of small and larger blood vessels is regularly encountered within chronic MS and is exemplified here with a staining for the protein collagen I.

shows loss of Zinc ions in chronic MS lesions and provides further information on the chemical nature of iron in MS brain tissue, which encompasses heme iron, ferrihydrite, magnetite and goethite.

VISUALIZATION OF IRON BY ULTRA-HIGH FIELD (7T) MRI

In addition, elevated iron content is seen in some active MS lesions, distinguishing them from lesions in patients with neuromyelitis optica (7). Upon the application of iron-sensitive sequences, 7T MRI turned out to be ideal for iron visualization in the brain tissue with high sensitivity and structural resolution *in vivo*. Information derived from gradient-echo sequences are generally used for these purposes and comprise T2*, susceptibility-weighted imaging (SWI) and quantitative susceptibility mapping (QSM). Although these modalities provide images reliably depicting iron content in basal ganglia and thalamus, the high amounts of myelin found in white matter prevent their straightforward application for white matter iron quantification (37). The reason is that diamagnetic myelin induces opposite local magnetic field changes, compared to paramagnetic iron. By comparing the reciprocal of T2*, i.e. R2*, and QSM with biochemical and histochemical iron determination in a post mortem study on unfixed human brains *in-situ*, we could show a good correlation between the biochemical or histochemical iron signal with quantification of the signal of both techniques in brain areas with low myelin content. However, in areas with high myelin content, QSM analysis turned out to be influenced by myelin and iron (Hametner *et al* 2018, in revision). Due to their high sensitivity, these MRI techniques have been recently used to address a number of questions related to vascular pathology or MS lesion structure and its dynamic evolution.

Relationship between MS lesions and cerebral veins

In contrast to histochemical iron stainings, susceptibility-sensitive MRI also depicts venous deoxygenated hemoglobin, allowing the creation of an anatomical vein atlas of the normal brain (20) and to show its alterations within MS lesions (12). The specificity of the signal for hemoglobin in intravascular erythrocytes can be documented in direct MRI-pathological correlation studies, but in such studies it has to be considered that all blood in the post mortem brain is de-oxygenated and therefore an erythrocyte-related signal is also seen in arteries. The presence of a central vein, which can be detected in high-field MRI, in MS lesions is a very characteristic finding (55), which helps to differentiate MS diagnostically from many (10, 54) but not all other inflammatory brain diseases (5). In addition, expansion of the perivascular Virchow Robin spaces was found to be associated with the degree of

brain atrophy, suggesting that such measurements may serve as an indicator for neurodegeneration (34).

Iron imaging of MS lesions—diffuse iron accumulation vs. loss

Neuropathological studies have demonstrated a loss of iron in the majority of active and inactive lesions, when compared to the surrounding NAWM (23,48). Putatively iron-sensitive MRI modalities such as phase imaging or QSM however have demonstrated an increase in phase (58) or susceptibility (8) in the majority of acute (58) or some chronic (8) MS lesions, which has been interpreted as iron accumulation, since MS lesions with iron accumulation indeed show hyperintensity in QSM (59). However, MS lesions show increase of phase or QSM also in the absence of iron accumulation and may even show it in the presence of lesional iron loss (57). Increased microstructural isotropy during MS lesion formation might explain this increase in MRI signal in lesions showing iron loss (60). Still, a subset of lesions was shown to accumulate iron across the lesion area (around 8% of WM lesions (23)) or at the lesion border (slowly expanding lesions, see below). A way to more specifically identify these two distinct morphological patterns of iron accumulation (nodular or ring-like iron accumulation) in MS lesions is the combination of gradient-echo T2* imaging with QSM (7). Applying this combination, 16.5% of MS lesions were classified as showing iron accumulation (7), which well matches neuropathological data.

Iron imaging of slowly expanding lesions

A number of recent Ultra-high field MRI studies have shown that a subset of lesion in patients with relapsing or progressive MS are characterized by the presence of a rim of high signal intensity of phase, R2* or QSM sequences (2, 4, 24, 25). The interpretation of these findings in relation to disease activity, however, was controversial. It was suggested that these are active lesions, associated with a rim of iron loaded macrophages at their margins (2). However, a longitudinal study showed that these rims were unchanged over an observation time of 2.5 years (4), thus arguing against their classification as active plaques. As discussed above, such iron rims are due to the accumulation of activated, iron-containing microglia at the plaque edge which show a pro-inflammatory phenotype (11). By morphological criteria they, thus, fulfill the criteria of slowly expanding lesions, but the iron rim forms in lesions, when they are located in a brain area with high iron content. Iron rims were very sparse or absent around inactive or remyelinated lesions and even around classical active MS plaques. Using a combined approach of postmortem/MRI analysis together with an *in vivo* longitudinal study in MS patients, a number of remarkable findings became apparent. Iron rim lesions could be readily detected in post mortem and *in vivo* 7T MRI in MS patients. The presence of the iron rim was stable in individual lesions over an observation period of 3.5 years. Most importantly,

iron rim lesions on average increased in size, and some were observed to fuse with adjacent lesions. In contrast, lesions devoid of iron rims showed the tendency to shrink, possibly due to tissue atrophy in chronic lesions. However, these processes occurred at a very slow pace and it took an observation time of at least 3.5 years to find a significantly different volume evolution between rim and non-rim lesions. These data suggest that lesion growth in the progressive stage of MS is a very slow process. Despite that, the presence of iron rim lesions may become a para-clinical marker for disability progression, when evaluated in a large scale prospective clinical study.

Iron imaging to improve lesion detection in the cortical grey matter

Multiple sclerosis has for long been regarded as a disease leading to demyelinated plaques in the white matter. Although some neuropathological studies have described grey matter lesions before (6, 32), the introduction of sensitive immunohistochemical methods for the detection of myelin (46) revealed extensive demyelination in the cortex and in brain stem nuclei (21). Grey matter lesions are difficult to detect due to the low density of myelinated fibers and the very low thickness of cortical myelin sheaths. This is a major challenge in clinical MS research, since cortical lesions likely play a major role in disease progression, in particular in patients with PPMS or SPMS. With conventional MRI, cortico-subcortical and some larger intracortical lesions can be detected, which corresponds in sensitivity to myelin stainings prior to the use of sensitive immunocytochemical techniques (32). Thus, particularly subpial lesions, which are the most important and prominent lesions in patients with progressive disease (36), are nearly completely missed in MRI.

Some improvement in grey matter lesion detection has so far been achieved with Ultra-high field imaging at 7T (33). The MRI sequences which showed improved sensitivity and specificity for the detection of demyelination in the grey matter are T2WI (30, 43), iron-sensitive sequences such as R2* and quantitative susceptibility mapping (QSM) (29), MP2-RAGE (3) and MTR sequences (1). Scanning MS brain specimens at 9.4 Tesla under post mortem conditions, which allow extended scan times without any movement artefacts, leads to a nearly complete visualization of all neuropathologically identified grey matter lesions even with routine sequences such as T2 imaging (52). In addition, in this study quantitative associations suggested that in cortical grey matter T1 relaxation times may be a predictor of neuronal density, and T2 relaxation times of myelin content (and—secondarily—axons). Iron-sensitive sequences such as T2*/R2* are also suitable (47) and take advantage of the concomitant iron loss in cortical lesions, augmenting the lesion contrast induced by myelin loss (61). However, even at 7T, *in vivo* imaging is currently still far away from the ideal situation in post mortem scanning. *In vivo*, partial volume effects due to the vicinity of cerebrospinal fluid appears

to impair detection of subpial lesions. Ultra-high field MRI has already contributed to improved lesion detection in the grey matter, which highlights the importance of lesions and diffuse changes in the deep grey matter, as shown in neuropathological studies (21) as a substrate for neurological and cognitive dysfunction (18). Similarly, analysis of cortical lesion numbers or volume at 7T showed more accurate correlation with clinical deficit or cognitive disturbances, compared to results obtained at lower field strength (16, 26). An important innovation is the combination of lesion detection with Ultra-high field MRI with functional MRI studies (41) or positron emission tomography (PET) analysis (27). These studies underscore the importance of cortical lesions in the disturbance of the functional connectome in the brain and shed light on the dynamics of microglia activation in the cortex and deep grey matter of MS patients. Despite these important achievements, one has to be aware that until now even Ultra-high field MRI operating at 7T only detects the tip of the iceberg of cortical demyelination present in MS patients and this is particularly the case for subpial cortical lesions. However, there is rapid progress in the field and significant improvement of the current situation can be expected in the near future.

CONCLUSIONS

Iron accumulates in the human brain with aging and alterations in iron content and distribution in the MS brain are now well documented. It is unlikely that changes in iron metabolism play a causative role in MS, rather they appear to act as an amplification factor for demyelination and neurodegeneration, particularly in aging patients with progressive disease. Iron related changes in the MS brain are complex and likely depend on the source of iron (heme or non-heme iron), cell-type-specific expression patterns of iron transport molecules and their alterations in the demyelinating and neurodegenerative process. Iron load and its changes in pathological conditions of the central nervous system can be visualized *in vivo* by MRI, with Ultra-high field MRI (7 Tesla) being particularly useful. Recent data indicate that these novel MRI technologies may become useful for clinical differential diagnosis, as a prognostic marker in MS patients and as a tool to monitor the efficacy of treatments in clinical trials in patients, who have entered the progressive stage of the disease.

REFERENCES

1. Abdel-Fahim R, Mistry N, Mouglin O, *et al* (2014) Improved detection of focal cortical lesions using 7T magnetisation transfer imaging in patients with multiple sclerosis. *Mult Scler Relat Disord* 3:258–265.
2. Absinta M, Sati P, Gaitan MI, *et al* (2013) Seven-tesla phase imaging of acute multiple sclerosis lesions: a new window into the inflammatory process. *Ann Neurol* 74:669–678.

3. Beck ES, Sati P, Sethi V, *et al* (2018) Improved visualization of cortical lesions in multiple sclerosis using 7T MP2RAGE. *AJNR Am J Neuroradiol*
4. Bian W, Harter K, Hammond-Rosenbluth KE, *et al* (2013) A serial *in vivo* 7T magnetic resonance phase imaging study of white matter lesions in multiple sclerosis. *Mult Scler* **19**:69–75.
5. Blaabjerg M, Ruprecht K, Sinnecker T, *et al* (2016) Widespread inflammation in CLIPPERS syndrome indicated by autopsy and ultra-high-field 7T MRI. *Neurol Neuroimmunol Neuroinflamm* **3**:e226.
6. Brownell B, Hughes JT (1962) The distribution of plaques in the cerebrum in multiple sclerosis. *J Neurol Neurosurg Psychiatry* **25**:315–320.
7. Chawla S, Kister I, Wuerfel J, *et al* (2016) Iron and non-iron-related characteristics of multiple sclerosis and neuromyelitis optica lesions at 7T MRI. *AJNR Am J Neuroradiol* **37**:1223–1230.
8. Chen W, Gauthier SA, Gupta A, *et al* (2014) Quantitative susceptibility mapping of multiple sclerosis lesions at various ages. *Radiology* **271**:183–192.
9. Chiou B, Lucassen E, Sather M, Kallianpur A, Connor J (2018) Semaphorin4A and H-ferritin utilize Tim-1 on human oligodendrocytes: a novel neuro-immune axis. *Glia*
10. Cortese R, Magnollay L, Tur C, *et al* (2018) Value of the central vein sign at 3T to differentiate MS from seropositive NMOSD. *Neurology* **90**:e1183–e1190.
11. Dal-Bianco A, Grabner G, Kronnerwetter C, *et al* (2017) Slow expansion of multiple sclerosis iron rim lesions: pathology and 7 T magnetic resonance imaging. *Acta Neuropathol* **133**:25–42.
12. Dal-Bianco A, Hametner S, Grabner G, *et al* (2015) Veins in plaques of multiple sclerosis patients—a longitudinal magnetic resonance imaging study at 7 Tesla. *Eur Radiol* **25**:2913–2920.
13. Damasceno FC, Condeles AL, Lopes AKB, *et al* (2018) The labile iron pool attenuates peroxynitrite-dependent damage and can no longer be considered solely a pro-oxidative cellular iron source. *J Biol Chem*
14. Duck KA, Simpson IA, Connor JR (2017) Regulatory mechanisms for iron transport across the blood-brain barrier. *Biochem Biophys Res Commun* **494**:70–75.
15. Dunham J, Bauer J, Campbell GR, *et al* (2017) Oxidative Injury and Iron Redistribution Are Pathological Hallmarks of Marmoset Experimental Autoimmune Encephalomyelitis. *J Neuropathol Exp Neurol* **76**:467–478.
16. Fartaria MJ, Bonnier G, Roche A, *et al* (2016) Automated detection of white matter and cortical lesions in early stages of multiple sclerosis. *J Magn Reson Imaging* **43**:1445–1454.
17. Frischer JM, Weigand SD, Guo Y, *et al* (2015) Clinical and pathological insights into the dynamic nature of the white matter multiple sclerosis plaque. *Ann Neurol* **78**:710–721.
18. Fujiwara E, Kmech JA, Cobzas D, *et al* (2017) Cognitive implications of deep gray matter iron in multiple sclerosis. *AJNR Am J Neuroradiol* **38**:942–948.
19. Gozzelino R, Jeney V, Soares MP (2010) Mechanisms of cell protection by heme oxygenase-1. *Annu Rev Pharmacol Toxicol* **50**:323–354.
20. Grabner G, Dal-Bianco A, Hametner S, Lassmann H, Trattnig S (2014) Group specific vein-atlasing: an application for analyzing the venous system under normal and multiple sclerosis conditions. *J Magn Reson Imaging* **40**:655–661.
21. Haider L, Simeonidou C, Steinberger G, *et al* (2014) Multiple sclerosis deep grey matter: the relation between demyelination, neurodegeneration, inflammation and iron. *J Neurol Neurosurg Psychiatry* **85**:1386–1395.
22. Hallgren B, Sourander P (1958) The effect of age on the non-haemin iron in the human brain. *J Neurochem* **3**:41–51.
23. Hametner S, Wimmer I, Haider L, Pfeifenbring S, Bruck W, Lassmann H (2013) Iron and neurodegeneration in the multiple sclerosis brain. *Ann Neurol* **74**:848–861.
24. Hammond KE, Metcalf M, Carvajal L, *et al* (2008) Quantitative *in vivo* magnetic resonance imaging of multiple sclerosis at 7 Tesla with sensitivity to iron. *Ann Neurol* **64**:707–713.
25. Harrison DM, Li X, Liu H, *et al* (2016) Lesion heterogeneity on high-field susceptibility MRI is associated with multiple sclerosis severity. *AJNR Am J Neuroradiol* **37**:1447–1453.
26. Harrison DM, Roy S, Oh J, *et al* (2015) Association of cortical lesion burden on 7-T magnetic resonance imaging with cognition and disability in multiple sclerosis. *JAMA Neurol* **72**:1004–1012.
27. Herranz E, Gianni C, Louapre C, *et al* (2016) Neuroinflammatory component of gray matter pathology in multiple sclerosis. *Ann Neurol* **80**:776–790.
28. Jiang R, Hua C, Wan Y, *et al* (2015) Hephaestin and ceruloplasmin play distinct but interrelated roles in iron homeostasis in mouse brain. *J Nutr* **145**:1003–1009.
29. Jonkman LE, Fleysher L, Steenwijk MD, *et al* (2016) Ultra-high field MTR and qR2* differentiates subpial cortical lesions from normal-appearing gray matter in multiple sclerosis. *Mult Scler* **22**:1306–1314.
30. Jonkman LE, Klaver R, Fleysher L, Inglese M, Geurts JJ (2015) Ultra-high-field MRI visualization of cortical multiple sclerosis lesions with T2 and T2*: a postmortem MRI and histopathology study. *AJNR Am J Neuroradiol* **36**:2062–2067.
31. Khalil M, Langkammer C, Pichler A, *et al* (2015) Dynamics of brain iron levels in multiple sclerosis: A longitudinal 3T MRI study. *Neurology* **84**:2396–2402.
32. Kidd D, Barkhof F, McConnell R, Algra PR, Allen IV, Revesz T (1999) Cortical lesions in multiple sclerosis. *Brain* **122**(Pt 1):17–26.
33. Kilsdonk ID, Jonkman LE, Klaver R, *et al* (2016) Increased cortical grey matter lesion detection in multiple sclerosis with 7 T MRI: a post-mortem verification study. *Brain* **139**:1472–1481.
34. Kilsdonk ID, Steenwijk MD, Pouwels PJ, *et al* (2015) Perivascular spaces in MS patients at 7 Tesla MRI: A marker of neurodegeneration? *Mult Scler* **21**:155–162.
35. Kristiansen M, Graversen JH, Jacobsen C, *et al* (2001) Identification of the haemoglobin scavenger receptor. *Nature* **409**:198–201
36. Kutzelnigg A, Lucchinetti CF, Stadelmann C, *et al* (2005) Cortical demyelination and diffuse white matter injury in multiple sclerosis. *Brain* **128**:2705–2712.
37. Langkammer C, Schweser F, Krebs N, *et al* (2012) Quantitative susceptibility mapping (QSM) as a means to measure brain iron? A post mortem validation study. *Neuroimage* **62**:1593–1599.
38. Li JY, Paragas N, Ned RM, *et al* (2009) Scara5 is a ferritin receptor mediating non-transferrin iron delivery. *Dev Cell* **16**:35–46.

39. Lopes KO, Sparks DL, Streit WJ (2008) Microglial dystrophy in the aged and Alzheimer's disease brain is associated with ferritin immunoreactivity. *Glia* **56**:1048–1060.
40. Mahad DH, Trapp BD, Lassmann H (2015) Pathological mechanisms in progressive multiple sclerosis. *Lancet Neurol* **14**:183–193.
41. Mangeat G, Badji A, Ouellette R, *et al* (2018) Changes in structural network are associated with cortical demyelination in early multiple sclerosis. *Hum Brain Mapp* **39**:2133–2146.
42. Mehta V, Pei W, Yang G, *et al* (2013) Iron is a sensitive biomarker for inflammation in multiple sclerosis lesions. *PLoS ONE* **8**:e57573.
43. Nielsen AS, Kinkel RP, Madigan N, Tinelli E, Benner T, Mainero C (2013) Contribution of cortical lesion subtypes at 7T MRI to physical and cognitive performance in MS. *Neurology* **81**:641–649.
44. Nielsen AS, Kinkel RP, Tinelli E, Benner T, Cohen-Adad J, Mainero C (2012) Focal cortical lesion detection in multiple sclerosis: 3 Tesla DIR versus 7 Tesla FLASH-T2. *J Magn Reson Imaging* **35**:537–542.
45. Obusez EC, Lowe M, Oh SH, *et al* (2018) 7T MR of intracranial pathology: Preliminary observations and comparisons to 3T and 1.5T. *NeuroImage* **168**:459–476.
46. Peterson JW, Bo L, Mork S, Chang A, Trapp BD (2001) Transected neurites, apoptotic neurons, and reduced inflammation in cortical multiple sclerosis lesions. *Ann Neurol* **50**:389–400.
47. Pitt D, Boster A, Pei W, *et al* (2010) Imaging cortical lesions in multiple sclerosis with ultra-high-field magnetic resonance imaging. *Arch Neurol* **67**:812–818.
48. Popescu BF, Frischer JM, Webb SM, *et al* (2017) Pathogenic implications of distinct patterns of iron and zinc in chronic MS lesions. *Acta Neuropathol* **134**:45–64.
49. Qureshi AI, Tuhim S, Broderick JP, Batjer HH, Hondo H, Hanley DF (2001) Spontaneous intracerebral hemorrhage. *N Engl J Med* **344**:1450–1460.
50. Schaer DJ, Vinchi F, Ingoglia G, Tolosano E, Buehler PW (2014) Haptoglobin, hemopexin, and related defense pathways—basic science, clinical perspectives, and drug development. *Front Physiol* **5**:415.
51. Schmalbrock P, Prakash RS, Schirda B, *et al* (2016) Basal ganglia iron in patients with multiple sclerosis measured with 7T quantitative susceptibility mapping correlates with inhibitory control. *AJNR Am J Neuroradiol* **37**:439–446.
52. Schmierer K, Parkes HG, So PW, *et al* (2010) High field (9.4 Tesla) magnetic resonance imaging of cortical grey matter lesions in multiple sclerosis. *Brain* **133**:858–867.
53. Schuh C, Wimmer I, Hametner S, *et al* (2014) Oxidative tissue injury in multiple sclerosis is only partly reflected in experimental disease models. *Acta Neuropathol* **128**:247–266.
54. Sinnecker T, Schumacher S, Mueller K, *et al* (2016) MRI phase changes in multiple sclerosis vs neuromyelitis optica lesions at 7T. *Neurol Neuroimmunol Neuroinflamm* **3**:e259.
55. Tallantyre EC, Morgan PS, Dixon JE, *et al* (2009) A comparison of 3T and 7T in the detection of small parenchymal veins within MS lesions. *Invest Radiol* **44**:491–494.
56. Vercellino M, Masera S, Lorenzatti M, *et al* (2009) Demyelination, inflammation, and neurodegeneration in multiple sclerosis deep gray matter. *J Neuropathol Exp Neurol* **68**:489–502.
57. Wiggermann V, Hametner S, Hernandez-Torres E, *et al* (2017) Susceptibility-sensitive MRI of multiple sclerosis lesions and the impact of normal-appearing white matter changes. *NMR Biomed* **30**.
58. Wiggermann V, Hernandez Torres E, Vavasour IM, *et al* (2013) Magnetic resonance frequency shifts during acute MS lesion formation. *Neurology* **81**:211–218.
59. Wisnieff C, Ramanan S, Olesik J, Gauthier S, Wang Y, Pitt D (2015) Quantitative susceptibility mapping (QSM) of white matter multiple sclerosis lesions: Interpreting positive susceptibility and the presence of iron. *Magn Reson Med* **74**:564–570.
60. Yablonskiy DA, Luo J, Sukstanskii AL, Iyer A, Cross AH (2012) Biophysical mechanisms of MRI signal frequency contrast in multiple sclerosis. *Proc Natl Acad Sci U S A* **109**:14212–14217.
61. Yao B, Hametner S, van Gelderen P, *et al* (2014) 7 Tesla magnetic resonance imaging to detect cortical pathology in multiple sclerosis. *PLoS ONE* **9**:e108863.
62. Yao B, Ikonomidou VN, Cantor FK, Ohayon JM, Duyn J, Bagnato F (2015) Heterogeneity of multiple sclerosis white matter lesions detected with T2*-weighted imaging at 7.0 Tesla. *J Neuroimaging* **25**:799–806.
63. Zrzavy T, Hametner S, Wimmer I, Butovsky O, Weiner HL, Lassmann H (2017) Loss of “homeostatic” microglia and patterns of their activation in active multiple sclerosis. *Brain* **140**:1900–1913.